CDF/PUB/QCD/PUBLIC/10084

Hyperon (Λ^0, $\overline{\Lambda}^0$, $\Xi^{+/-}$ and $\Omega^{+/-}$) Production in $\bar{p}p$ collisions at $\sqrt{s}$ = 1.96 TeV.

The CDF Collaboration
URL http://www-cdf.fnal.gov
(Dated: February 15, 2010)

Abstract

We report on the measurements of inclusive invariant p_T differential cross section of centrally produced hyperons ($|\eta|$ <1) from minimum biased events taken at the Fermilab Tevatron collider. The invariant differential cross sections are also presented for different multiplicity intervals.

Introduction

Ever since the discovery of strange particles from cosmic ray interactions [1], particles containing strange quarks have been a subject of numerous studies because they could reveal the particle production mechanism from the collision. The interest in these particles increased with the invention of quark-gluon plasma (QGP), which is expected to be produced when a large amount of energy and particles are deposited in a small volume. If a QGP is formed, then one of its signatures could be enhanced production of strange particles such as kaons and hyperons.

There is ample data on the particles with one strange quark, but very little data on the production of doubly charged particles exists [3,4]. The studies of lambdas and cascades from colliders such as $Sp\bar{p}S$ [5] and Tevatron [6,7] are also very limited in terms of statistics and p_T ranges and omega data does not exist. In this paper, based on ~100 million minimum biased events collected with the CDF II detector, the inclusive invariant p_T differential cross sections of these are measured up to 10 GeV/c p_T . The CDF detector is described in detail in [8]. The main detector for this analysis is the tracking element consisting of the COT and Silicon Detector. Because the COT is a low mass detector, it is well suited for these types of studies.

Data, Event and Track Selection

The data is collected with the minimum biased trigger between March 2002 and February 2008. Events with a good vertex between -60 and 60 cm are chosen. When an event has more than one good vertex, the highest quality vertex is chosen and it is required that there are no other vertices within +/- 5 cm of the vertex. Tracks are selected with χ^2/dof < 2.5 and at least two good COT axial and stereo segments. Because of low tracking efficiency of very low momentum tracks, only tracks with p_T > 0.3 GeV/c are used in this analysis. The default p_T cut is 0.325 GeV/c and 0.3 GeV/c is to study the effect of the p_T cut.

Analysis

The first step of the lambda (Λ^0 and $\overline{\Lambda}^0$) reconstruction is to take two oppositely charged tracks with p_T > 0.325 GeV/c and calculate their intersecting coordinate in the r-ϕ plane (the secondary vertex). Once the intersection point is found, the Z coordinate of each track (Z_1 and Z_2) is calculated at that point. If the distance between the two is less than 1.5 cm, they are combined and swam back to the beam line and compared with the event vertex. If the closest distance (d0) to the vertex in the r-ϕ plane is less than 0.25 cm and the difference (δZ_0) between the pair Z and the event Z vertex position is less than 2.0 cm, the pair is accepted. In order to reduce the background further, it is also required that the distance between the event vertex and the secondary vertex be greater than 2.5 cm. This is the decay length (L_Λ) in the r-ϕ plane. The invariant mass of the pair is calculated by assigning the proton mass to the track with higher $p_{T.}$ and the pion mass to the other. This is kinematically true. Figure 1 shows the pπ invariant mass

for pairs (lambda candidates) with $|\eta| < 1$ corresponds to the COT acceptance. The peak does not fit well with a single Gaussian function and a double Gaussian function with third degree polynomial is used [9].

In order to calculate the inclusive p_T distribution, the invariant mass is divided into many p_T intervals. The number of lambdas from each plot is obtained by fitting the plot with a Gaussian function for the peak and third degree polynomial function for the background. If the fit is good, the polynomial background is subtracted, and the number of lambdas in this p_T interval is the sum of entries within the lambda mass window cut (1.111 to 1.121 GeV/c^2). This number is acceptance corrected to obtain the differential p_T cross section. For the acceptance calculation as a function of p_T, two sets of MC data are generated. One set mixes a lambda with fixed p_T to one PYTHIA minimum biased events [10], and the other mixes the same to four PYTHIA minimum biased events. In this case the four is the average of a Poisson distribution. The default acceptance values are from the latter and the difference of the two is one of the systematic errors as discussed later. The difference of the two is in mainly $p_T < 2$ GeV/c region.

To calculate the inclusive invariant p_T differential cross section, the total cross section corresponding to the minimum biased trigger is taken from the previously published Ks paper [11]. The value is increased by 1 mb to 44mb+/-6 mb to take into account the center of mass energy difference from 1.8 to 1.96 TeV [12]. Figure 2 shows our result. The error bars include the systematic errors.

There are two main contributions to the systematic errors. One is from fitting the invariant mass distribution and the other is the acceptance calculation. The systematic error due to fitting is only important when the background cannot be fitted well. For lambdas, this situation arises for the plots with $p_T < 1.4$ GeV/c. Because of the track p_T cut, the background rises quickly near the lambda peak and is difficult to parameterize. The acceptance systematic error as a function of p_T is calculated by changing the default cut values. The first one is the number of mixed minimum biased PYTHIA events as mentioned earlier. Others are p_T cut changed to >0.3 and >0.35 GeV/c, $|Z_1-Z_2|$ changed to 1and <2 cm, d0 changed to <0.10, δZ_0 changed to <1.5 and <5 cm and L_Λ changed to >1 and >5 cm. For each variation, the new acceptance curve is obtained and the invariant differential distribution is re-calculated. The new distribution is divided by the same obtained with default cuts. This ratio ($R_j(p_T)$) is subtracted from one to get the difference with respect to the default distribution, where j indicates a variation. The total systematic error at a p_T is the square root of the quadratic sum of ($R_j(p_T)$-1). The systematic errors vary from about 25% (p_T~1 GeV/c) to 10% (p_T~2.0 GeV/c), then level off and slightly increase to 15% (p_T> 7 GeV/c).

The inclusive p_T differential cross section is fitted with a power law function, $(A)(p_0)^n/(p_T + p_0)^n$. In order to compare with the previous Ks result, p_0 is fixed at 1.3GeV/c. Table 1 shows the results. The data deviates from the curve below p_T ~ 2 GeV/c. This is true even if p_0 is floated. For the low p_T region, the data fits better with an exponential function, $B\exp(-bp_T)$ and the fitted values are in Table 2. The slope, b, is not inconsistent with previous measurements [6,7].

	Ks (Run I published)	Lambda $2<p_T<10$ GeV/c	Cascade $2<p_T<10$ GeV/c	omega $2<p_T<10$ GeV/c
A (mb/GeV^2 c^3)	45+/-9	170+/-12	1.44+/-0.27	1.35+/-0.60
A' (at p_T =2 GeV/c)		(4.9+/-0.13)x10^{-2}	(7.0+/-0.4)x10^{-3}	(7.9+/-1.2)x10^{-4}
n	7.7+/-0.2	8.7+/-0.04	8.20+/-0.14	7.9+/-0.32
χ^2/dof	8.1/11	22.1/15	16.8/15	9.6/8

Table 1. The results of the fit to the inclusive differential cross section with the power law function for $p_T > 2$ GeV/c with p_0 =1.3. The K_s fit values are from [10] at 1.8 TeV. The errors on A do not include the cross section error.

	Lambda $1.2<p_T<2$ GeV/c	Lambda $1.2<p_T<4$ GeV/c	Cascade $1.5<p_T<4$ GeV/c	Omega $2<p_T<4$ GeV/c
B (mb/GeV^{2}c^3)	4.9+/-1.0	3.33+/-0.20	0.156+/-0.043	0.021+/-0.010=1
b (GeV^{-1})	2.30+/-0.13	2.10+/-0.02	1.73+/-0.10	1.75+/-0.15
χ^2/dof	3.5/4	18.7/12	3.0/8	5.3/3

Table 2. The results of the fit to the inclusive differential cross section with an exponential function. The errors on B do not include the cross section error.

The cascade (Ξ^- and Ξ^+) reconstruction decay mode is $\Xi^- \rightarrow \Lambda\pi^- \rightarrow (p\pi^+)\pi^-$. Lambdas previously constructed are used to reconstruct cascades. First the lambda candidates within the invariant mass 1.111 and 1.121 GeV/c are chosen before d0 and δZ_0 cuts are applied. This is because some lambdas from cascades may miss the vertex cuts. For each lambda candidate, the coordinate of the intersection point between the candidate and another track (third track) is calculated in r-ϕ space. Once the intersection point is found, the Z coordinates are calculated at the point (Z_3 for the third track and Z_4 for lambda candidate). If the distance between the two ($|Z_3-Z_4|$) is less than 1.5 cm the candidate and the third track are combined and swam back to the beam line and compared with the event vertex. Before combining the two, the mass of the lambda candidate is fixed to the lambda mass (1.1157 GeV/c^2) [13] and the third track is assigned the pion mass. There are two decay lengths for cascades. One is the lambda decay length and the other is the cascade decay length. We require that the lambda decay length to be greater than 2.5 cm and cascade decay length (L_Ξ) to be greater than 1cm. Moreover, since lambdas are from cascades, we also require the difference between the lambda decay length and cascade decay length to be greater than 0.5 cm. The final cut is the event vertex cut. Similar to the lambda case, d0 of the $p\pi\pi$ pair is less than 0.25 cm and the distance to the event Z vertex is less than 2.0 cm. These are the cascade candidates.

The invariant mass of cascade candidates is plotted in Figure 1. Like the lambda case, the plot is divided into several p_T intervals and fitted with a Gaussian plus a polynomial function. The number of cascades is the sum of entries from 1.31 to 1.33 GeV/c^2 after the polynomial background is subtracted. This number is acceptance corrected (average of cascade and anti-cascade acceptance) and the inclusive invariant differential cross section is shown in Figure 2. The systematic errors are estimated similarly to the Λ case with one additional variation, L_Ξ (to 3.0 cm). The final systematic error is ~15% at p_T ~ 2 GeV/c and levels off at ~10% for p_T >4 GeV/c. The contribution to the systematic errors due to the fitting is quite small because the background is well parameterized with the polynomial function. The inclusive invariant p_T distribution is also fitted with a power law function with a fixed p_0. The fitted parameters are shown in Table 1. Data with p_T < 4 GeV/c, are fitted with an exponential function and the fit values are listed in Table 2.

The omega (Ω^- and Ω^+) reconstruction is identical to the cascade reconstruction except the kaon mass is assigned to the third track. The number of omegas as a function of p_T is calculated differently from lambdas and cascades. For omegas, before fitting the $p\pi K$ invariant mass distribution with a Gaussian and Polynomial, the background distribution obtained from the outside lambda mass region (side bands) at the same p_T interval is subtracted. The side bands are $1.095<M_{p\pi}< 1.105$ GeV/c^2 and $1.127<M_{p\pi}< 1.137$ GeV/c^2. The side band background is normalized (scale factor) to the mass region ($1.69<M_{p\pi K}<1.74$ GeV/c^2). The subtracted invariant mass for all p_T is shown in Figure 1. The number of omegas for several p_T intervals is calculated like the cascade case with the mass window 1.665 to 1.68 GeV/c^2. Although the background subtraction is not really necessary, the fits are generally better. The number of omegas is re-calculated after reducing the scale factor by 20% and the difference is put into the systematic errors. The omega p_T distribution is shown in Figure 2 and the fit results with fixed p_0 are tabulated in Table 1 and Table 2 has the fit results with an exponential function (p_T < 4 GeV/c). Because of low statistics, the systematic error from each variation is dominated by fitting and background subtraction error. For this reason, the cascade systematic error as a function of p_T is used after adding the background subtraction contribution.

The right plot in Figure 2 shows the ratio of Ξ/Λ and Ω/Λ as a function of p_T. For the Ξ/Λ ratio, there is a gentle rise at the beginning and the ratio plateaus out at higher p_T region. We should note that the lambdas include the lambdas from sigmas ($\Sigma \rightarrow \Lambda\gamma$) and cascades ($\Xi^{+/-}$,$\Xi^0$ and $\overline{\Xi}^0$). Because of a very short Σ life time, the lambdas from sigmas cannot be separated out. Some of the lambdas from cascades are removed because of the vertex cut. Cascade MC data shows that ~50% of lambdas from cascades pass the d0 and δZ cuts and the fraction is fairly independent of cascade p_T. The ratio plots are fitted with a constant and Ξ/Λ=0.17+/-0.1 and Ω/Λ=0.025+/-0.02 are obtained.

Figure 4 shows the inclusive p_T distributions for two different multiplicity regions, N_{ch} < 10 and N_{ch} >24. N_{ch} is the number of reconstructed good tracks with $|\eta|$ <1, p_T > 0.3 GeV/c, d0 < 0.25 cm and δZ < 2.0 cm. N_{ch} =24 (10) corresponds to $dN/d\eta$ ~16 (7) including the unseen tracks less than 0.3 GeV/c and track reconstruction efficiency [14]. Only Λ and Ξ plots are shown because of low Ω statistics. There are more high p_T particles in high multiplicity events.

In summary, the production properties of lambdas, cascades and omegas from minimum biased events at 1.96 TeV center of mass energy are studied. The production ratio of three particles as a function of p_T is fairly constant and for events with high multiplicity, the p_T slope is lower compared to events with low multiplicity.

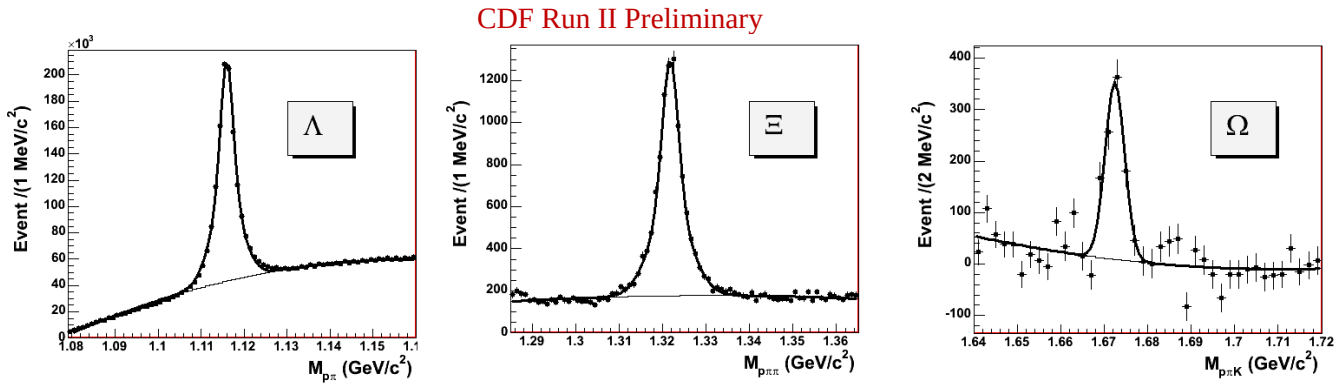

Figure 1. The invariant mass of pπ (left), pππ (center) and pπK (right) combination. The solid curves are fitted curves, a double Gaussian for Λ and Ξ and a Gaussian for Ω plus third degree polynomial for the background.

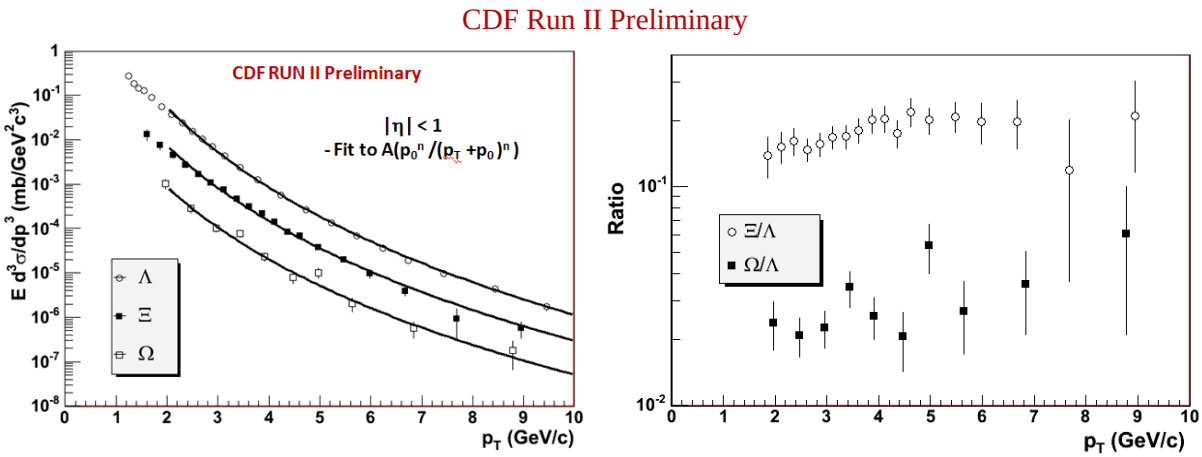

Figure 2. Left plot: Inclusive invariant p_T distribution for Λ, Ξ and Ω within |η|<1. The solid curves are from fit to the functional form $(A)(p_0)^n/(p_T+p_0)^n$ with p_0 =1.3. See Table 1 for the fitted parameters. Right plot: The ratio of Ξ/Λ and Ω/Λ as a function of p_T.

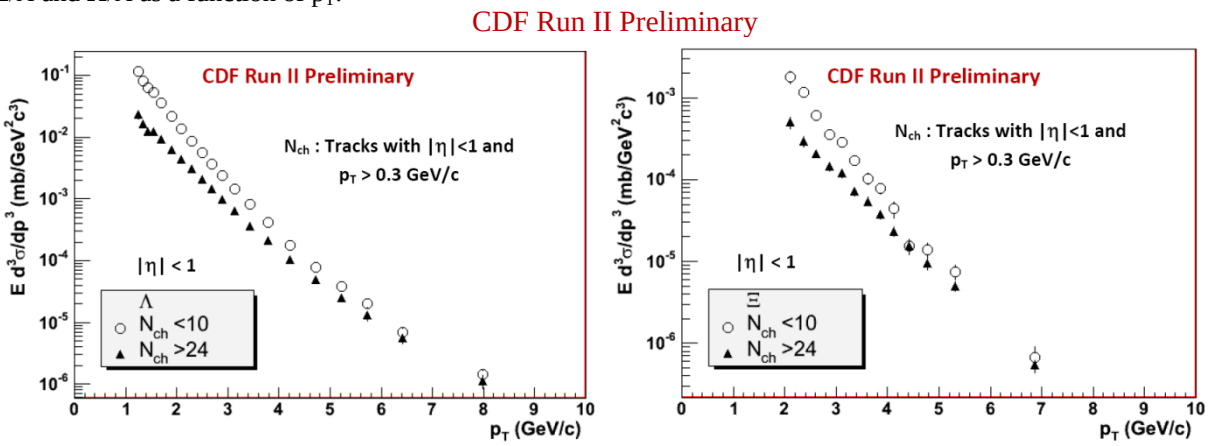

Figure 3. The inclusive p_T distributions for two different multiplicity regions, N_{ch} < 10 and N_{ch} >24. Left plot is for lambdas and right plot is for cascades.

Acknowledgments

We thank the Fermilab staffs and the technical staffs of the participating institutions for their vital contributions. This work was supported by the U.S. Department of Energy and National Science Foundation; the Italian Istituto Nazionale di Fisica Nucleare; the Ministry of Education, Culture, Sports, Science and Technology of Japan; the Natural Sciences and Engineering Research Council of Canada; the National Science Council of the Republic of China; the Swiss National Science Foundation; the A.P. Sloan Foundation; the Bundesministerium fur Bildung und Forschung, Germany; the Korean Science and Engineering Foundation and the Korean Research Foundation; the Science and Technology Facilities Council and the Royal Society, UK; the Institut National de Physique Nucleaire et Physique des Particules/CNRS; the Russian Foundation for Basic Research; the Ministerio de Educaci _on y Ciencia and Programa Consolider-Ingenio 2010, Spain; the Slovak R&D Agency; and the Academy of Finland.

References

[1] G.Rochester and C. Butler, Nature 160, 855 (1947)

[3] M. Bourquin *et al*., Z Phys, C5, 275 (1980)

[4] T. Akesson *at al*., Nucl. Phys. B249, 1(1984)

[5] G. Alner *et al*., Phys. Lett. 151B, 309 (1985)

[6] S. Banerjee *et al.*, Phys. Rev. Lett. 62, 12 (1989)

[7] T. Alexopoulos *et al*., Phys. Rev. D46, 2773 (1992)

[8] F. Abe *et al.*, Nucl. Instrum. Methods Phys. Res. A 271, 387 (1988); D. Amidei, et al., Nucl. Instum. Methods Phys. Res. A 350, 73 (1994); F. Abe *et al.*, Phys. Rev. D 52, 4784 (1995); P. Azzi *et al*., Nucl. Instrum. Methods Phys. Res. A 360, Report, Fermilab-Pub-96/390-E

[10] The reason why a single Gaussian does not fit well is due to mixing tracks from wide range of p_T values and resolution. The double Gaussian mass peak is well reproduced with MC data.

[9]T. Sjostrand *et al*., High-Energy-Physics Event Generation with PYTHIA 6.1, Comput. Phys. Commun. 135, 238 (2001).

[11] F. Abe *et al*., Phys. Rev. D40, 3791 (1989)

[12] G.Alner *et a*l., Z Physik C. 32, 153 (1986)

[13] C. Amsler *et al.* (Particle Data Group), Physics Letters B667**,** 1 (2008)

[14] F. Abe *et al.*, Phys. Rev. Lett. 61, 1819 (1988